# Multiparticle configurations in $N = 84$ isotones located at the proton drip line

D. Seweryniak,[1,2] J. Uusitalo,[1] P. Bhattacharyya,[3] M. P. Carpenter,[1] J. A. Cizewski,[1,4] K. Y. Ding,[4,*] C. N. Davids,[1] N. Fotiades,[4,†] R. V. F. Janssens,[1] T. Lauritsen,[1] C. J. Lister,[1] A. O. Macchiavelli,[5] D. Nisius,[1] P. Reiter,[1] W. B. Walters,[2] and P. J. Woods[6]

[1]*Argonne National Laboratory, Argonne, Illinois 60439, USA*
[2]*University of Maryland, College Park, Maryland 20742, USA*
[3]*Purdue University, West Lafayette, Indiana 47907, USA*
[4]*Rutgers University, New Brunswick, New Jersey 08903, USA*
[5]*Lawrence Berkeley Laboratory, California 94720, USA*
[6]*University of Edinburgh, Edinburgh, EH9 3JZ United Kingdom*

(Received 11 February 2005; published 26 May 2005)

Excited states in the proton-rich $N = 84$ isotones $^{156}_{72}Hf_{84}$, $^{157}_{73}Ta_{84}$, and $^{158}_{74}W_{84}$ were observed using $^{102}Pd(^{58}Ni, xp2n)$ reactions at 270 MeV. $\gamma$ rays were detected with the Gammasphere array of Compton-suppressed Ge detectors coupled with the Argonne fragment mass analyzer and were assigned to individual reaction channels using the recoil-decay tagging method. Prompt $\gamma$-ray cascades were associated with the $\alpha$ decay of both the ground state and the $8^+$ isomeric state in $^{156}Hf$, the $h_{11/2}$ state in $^{157}Ta$, and the $8^+$ isomeric state in $^{158}W$. The level schemes constructed for $^{156}Hf$, $^{157}Ta$, and $^{158}W$ are compared with these of lighter $N = 84$ isotones and are discussed within the framework of the shell model.

DOI: 10.1103/PhysRevC.71.054319 PACS number(s): 23.20.Lv, 27.70.+q

## I. INTRODUCTION

The structure of nuclei close to the $N = 82$ neutron shell closure, above the $Z = 64$ line, have for a long time been the aim of numerous studies. Interest in this region of the chart of nuclides was motivated by the discovery that $^{146}_{64}Gd_{82}$ can be regarded as a doubly magic nucleus [1]. This has been attributed to the presence of a large energy gap between the $g_{7/2}$, $d_{5/2}$ proton orbitals, which are filled in $^{146}Gd$, and the remaining proton orbitals of the $Z = 50$–82 major shell (i.e., $h_{11/2}$, $s_{1/2}$, and $d_{3/2}$). The immediate neighbors of $^{146}Gd$ can be produced with relatively large cross sections using heavy-ion induced fusion-evaporation reactions. Based on a large body of data, single-particle energies and two-body matrix elements with respect to the $^{146}Gd$ core were deduced in Ref. [2]. Several shell-model calculations using these parameters successfully reproduce excited states observed in nuclei with more than two valence nucleons outside the $^{146}Gd$ core [2,3].

The $N = 82$ isotones heavier than $^{146}_{64}Gd_{82}$ are an ideal ground for studying proton-proton residual interactions. Yrast states in these nuclei can be accurately described using the $(\pi h_{11/2})^n$ configuration space. Conversely, the $N = 84$ isotones heavier than $^{148}_{64}Gd_{84}$ are crucial for determining both the interaction between neutrons occupying the lowest $f_{7/2}$ and $h_{9/2}$ orbitals, and the interaction between these neutrons and protons gradually filling the $h_{11/2}$ orbital. In addition, the $i_{13/2}$ neutron orbital plays a significant role at higher excitation energies, where it contributes efficiently to the total spin because of its large intrinsic angular momentum. The $3^-$ state in $^{146}Gd$ is situated at only 1597 keV. As a result, many excited states contain also a sizable octupole phonon component.

Another interesting aspect of nuclei with $N \geqslant 82$ and $Z \geqslant 64$ is the close proximity of the proton drip line. A number of proton emitters have been identified in this region in a series of experiments performed at the ATLAS accelerator using the Argonne Fragment Mass Analyzer [4]. Every odd-$Z$ element between Ta and Bi has been found to have at least one isotope decaying by proton emission. In addition, many nuclei in this region $\alpha$ decay (see Ref. [5] and references therein).

Studies of proton-rich nuclei close to $N \geqslant 82$, with $Z > 64$ are hampered by very small production cross sections, because of the lack of suitable stable target and beam combinations, strong competition from fission, and fragmentation of the fusion-evaporation reactions. The $^{154}_{72}Hf_{82}$ nucleus is the heaviest $N = 82$ isotone with known excited states. The decay of its $10^+$ isomer has been observed using the Daresbury Recoil Separator [6]. Excited states of even-even $N = 84$ isotones through $^{154}_{70}Yb_{84}$ [7] and odd-$Z$, $N = 84$ isotones through $^{153}_{69}Tm_{84}$ [8] have been investigated in a series of in-beam experiments summarized in Ref. [3].

In the present work, prompt $\gamma$-ray cascades correlated with $\alpha$ lines assigned previously to $^{156}Hf$, $^{157}Ta$, and $^{158}W$ were identified using the recoil-decay tagging (RDT) method. This is a continuation of an earlier measurement carried out with the AYEBALL Ge array [9]. The results on excited states in $^{155}Yb$ and $^{155,156,157}Lu$ from the present experiment have already been reported in Ref. [10]. The experimental setup and the results are described in Sec. II. In Sec. III the level schemes obtained for $^{156}Hf$, $^{157}Ta$, and $^{158}W$ are compared with lighter $N = 84$ isotones and with shell-model calculations.

## II. EXPERIMENTAL RESULTS

A 270-MeV $^{58}Ni$ beam from the ATLAS accelerator was used to bombard a 1 mg/cm$^2$ $^{102}Pd$ target, enriched to

*Present address: Telecordia Technology, Piscataway, NJ 08854.
†Present address: Los Alamos Laboratory, Los Alamos, NM 87545.

 

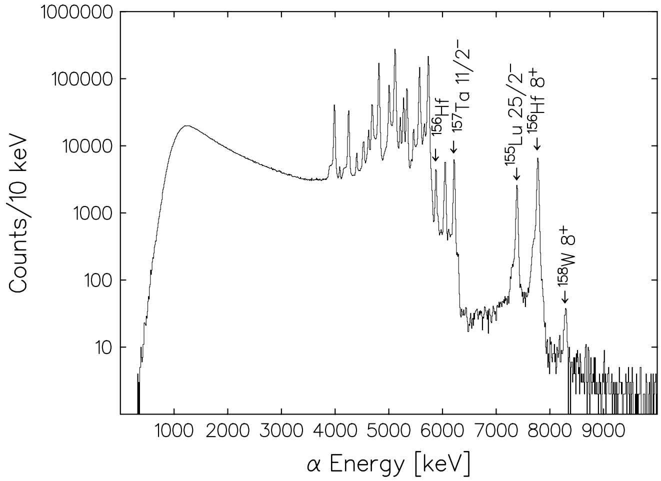


FIG. 1. The energy spectrum of $\alpha$ particles detected in the DSSD.

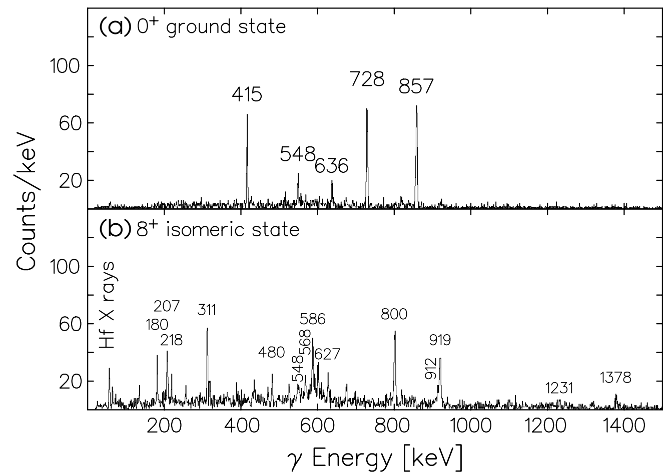


FIG. 2. $\gamma$-ray singles spectra correlated with (a) the ground state $\alpha$ decay of $^{156}$Hf and (b) the $\alpha$ decay of the $8^+$ isomeric state in $^{156}$Hf.

69%, to populate excited states in light $N = 84$ isotones via $xp2n$ fusion-evaporation channels. $\gamma$ rays were detected with the Gammasphere [11] array of Compton-suppressed HPGe detectors, in coincidence with the Argonne fragment mass analyzer (FMA) [12]. Detected $\gamma$ rays were assigned to individual reaction channels using the RDT method [13]. Recoiling nuclei were dispersed in the FMA according to their mass-to-charge state ratio and implanted into a 60-$\mu$m-thick, $16 \times 16\,\text{mm}^2$, $48 \times 48$-strip, double-sided silicon strip detector (DSSD) placed behind the focal plane. The subsequent characteristic $\alpha$ decays, observed in the same DSSD pixel as the implantation, allowed for the identification of the implanted residues and, thus, of the $\gamma$ rays detected at the target position in coincidence with the residues.

The energy spectrum of $\alpha$ particles collected in the DSSD during the experiment is shown in Fig. 1. The $\alpha$ spectrum is rather complex. Observed $\alpha$ lines were assigned to individual $A/Q$ values in the FMA and were identified based on their energies and half-lives. The lines associated with the $^{155}$Lu, $^{156}$Hf, $^{157}$Ta, and $^{158}$W nuclei are labeled in Fig. 1. These $\alpha$ lines represent about 1% of the entire spectrum.

$\gamma$-ray transitions correlated with individual $\alpha$ lines were ordered on the basis of $\gamma$-$\gamma$ coincidence relationships, as well as energy and intensity balance. $\gamma$-ray multipolarities were obtained from angular distributions. A maximum spin change was assumed for most of the observed $\gamma$-ray transitions, as is often the case in heavy-ion fusion evaporation reactions.

### A. The $^{156}$Hf nucleus

The ground state of $^{156}$Hf has an half life of 23 ms and is known to decay predominantly by emitting an $\alpha$ particle with an energy of 5.87 MeV. Another $\alpha$ line with an energy of 7.78 MeV and a half-life of 0.52 ms has been assigned to the decay of an isomeric state in $^{156}$Hf [5]. The isomeric state was populated in the $\beta$ decay of the $[\pi h_{11/2}\nu f_{7/2}]_{9^+}$ state in $^{156}$Ta, and, as a result, it was assigned the $[\nu h_{9/2}\nu f_{7/2}]_{8^+}$ configuration in analogy to lighter $N = 84$ isotones [14]. In the present experiment, prompt $\gamma$-ray cascades were correlated with both $^{156}$Hf $\alpha$ lines.

Singles $\gamma$-ray spectra tagged by the $^{156}$Hf $\alpha$ lines are presented in Fig. 2. The energies, intensities, and angular distribution ratios $R = I_\gamma(\approx 180^\circ)/I_\gamma(\approx 90^\circ)$ for $\gamma$ rays correlated with the $^{156}$Hf $\alpha$ decays are given in Table I. The spectrum associated with the ground-state $^{156}$Hf decay is dominated by three strong transitions. $\gamma$ rays in coincidence with the 415-, 728-, and 857-keV transitions are shown in Fig. 3. The three $\gamma$ rays are mutually coincident. Their angular distribution ratios are consistent with a stretched quadrupole character and they are proposed to form a $6^+ \to 4^+ \to 2^+ \to 0^+$ cascade. According to Fig. 3, the weaker 636- and 597-keV transitions feed the ground-state band at spin $6\hbar$ and $4\hbar$, respectively. The 857-keV coincidence gate reveals a 597-keV transition, which is proposed to feed the $2^+$ state.

The spectrum correlated with the $\alpha$ particles emitted from the isomeric state is more complex, indicating fragmentation of the decay paths. $\gamma$ rays in coincidence with the three strongest tramsitions at 919, 800, and 586 keV are shown in Fig. 4. These transitions are in mutual coincidence. Their angular distribution ratios are consistent with stretched quadrupole multipolarity and spins $10^+$, $12^+$, and $14^+$ are assigned to the 2896-, 3696-, and 4282-keV states, respectively. The 919-keV transition was placed at the bottom of the cascade because it is in coincidence with the 311-keV transition, which is not present in the 800- and 586-keV coincidence gates (see Fig. 4).

Based on the $\gamma\gamma$ coincidence relations, a side structure is proposed, which feeds into the yrast band at spin $8\hbar$ and $10\hbar$. The spin and parity assignments for the side band are discussed below. A level scheme for $^{156}$Hf is presented in Fig. 5, where only the strongest transitions were placed because of limited $\gamma\gamma$ statistics.

### B. The $^{157}$Ta nucleus

Three $\alpha$-emitting states have been associated with the decay of $^{157}$Ta. The strongest line, with an energy of 6213(4) keV and an half-life of 4.3(1) ms, was associated with the $h_{11/2}$ state, whereas a weaker line at 7744(8) keV with a 1.7(1) ms half-life

TABLE I. Energies, intensities, angular distribution ratios, and proposed assignments of the $\gamma$-ray transitions correlated with the $\alpha$ decay of the ground state and the $8^+$ isomeric state in $^{156}$Hf.

| Energy (keV) | Intensity | $R = I_\gamma(\approx 180^\circ)/I_\gamma(\approx 0^\circ)$ | $I^{\pi_i} \rightarrow I^{\pi}{}_f$ assignment |
|---|---|---|---|
| 415.0 | 35(3) | 1.06(25) | $6^+ \rightarrow 4^+$ |
| 547.6 | 20(2) | 1.92(66) | $(6_2^+) \rightarrow 6^+$ |
| 597 | | | $(2_2^+) \rightarrow 2^+$ |
| 636.4 | 18(3) | 0.67(29) | $(4_2^+) \rightarrow 4^+$ |
| 728.0 | 80(5) | 0.84(17) | $4^+ \rightarrow 2^+$ |
| 857.2 | 100(5) | 1.01(19) | $2^+ \rightarrow 0^+$ |
| 55.2 | 79(10) | | $K_\alpha$ X rays |
| 63.4 | 31(6) | | $K_\beta$ X rays |
| 133.5 | 12(2) | 1.55(66) | |
| 180.4 | 21(2) | 1.29(43) | $(14^+) \rightarrow (12_2^+)$ |
| 206.7 | 23(3) | 0.66(21) | |
| 208.5 | 10(2) | | |
| 218.0 | 12.6(17) | 1.20(47) | |
| 255.0 | 8.4(15) | | |
| 311.0 | 38(3) | 0.78(18) | $11^- \rightarrow 10^+$ |
| 317.3 | 13(2) | 0.51(19) | |
| 388.3 | 9.7(18) | | |
| 428.8 | 8.4(19) | | |
| 434.1 | 18(2) | | |
| 469.4 | 15(2) | | |
| 480.2 | 24(3) | 1.01(34) | $(12_2^+) \rightarrow (10_2^+)$ |
| 524.6 | 9(2) | | |
| 548.1 | 15(3) | | |
| 567.5 | 18(3) | | $(14^+) \rightarrow (12_2^+)$ |
| 579.3 | 10(3) | 0.90(33) | |
| 586.2 | 50(5) | 1.85(50) | $14^+ \rightarrow 12^+$ |
| 591.8 | 16(3) | 1.46(63) | |
| 600.4 | 26(4) | | |
| 626.5 | 17(3) | 2.29(73) | $(12_2^+) \rightarrow 11^-$ |
| 673.8 | 13(3) | | |
| 779.7 | 9(2) | | |
| 788.0 | 14(3) | | |
| 800.1 | 100(6) | 1.37(27) | $10^+ \rightarrow 8^+$ |
| 818.4 | 15(3) | | |
| 912.3 | 29(4) | | |
| 918.8 | 77(6) | 1.65(44) | $12^+ \rightarrow 10^+$ |
| 1230.7 | 15(3) | | $11^- \rightarrow 8^+$ |
| 1317.8 | 11(3) | | |
| 1378.0 | 25(4) | 1.12(40) | $(10_2^+) \rightarrow 8^+$ |

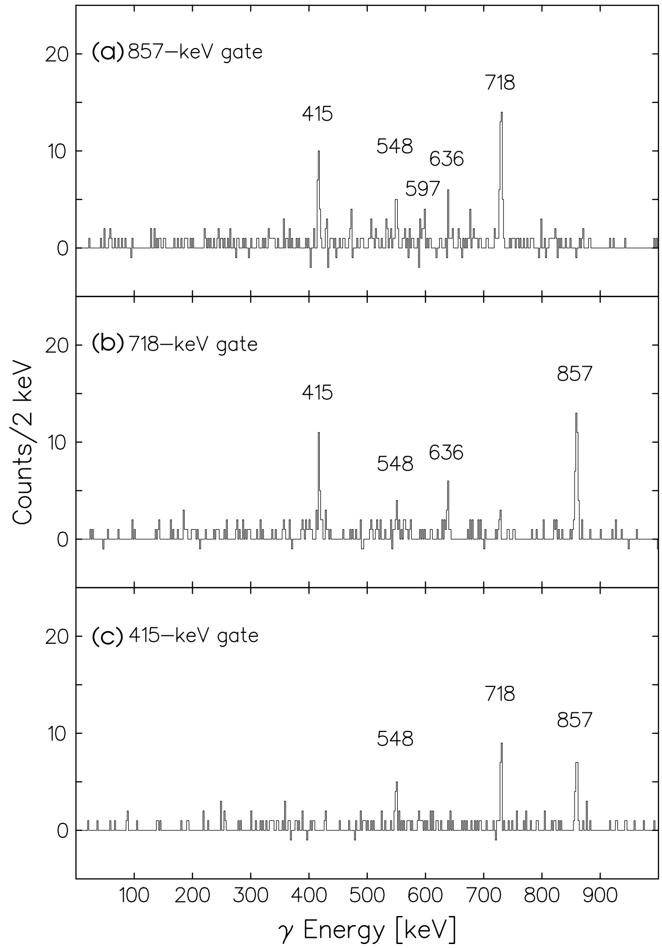


FIG. 3. $\gamma$-ray spectra in coincidence with the 857-, 718-, and 415-keV transitions tagged by the ground-state $\alpha$ decay in $^{156}$Hf.

was assigned to the $25/2^-$ high-spin isomer [5]. The third state, which was proposed to be the ground state, was found to decay via 6117(4)-keV $\alpha$ emission with half-life of 10.1(4) ms, and a weak 3.4(12)%, 927(7)-keV proton branch [15]. Based on the proton partial half-life, the ground state was interpreted as the $s_{1/2}$ state. The $h_{11/2}$ state was deduced to be located 22(5) keV about the $s_{1/2}$ ground state [15].

The ground state and the $h_{11/2}$ isomer $\alpha$ lines were observed in the present experiment. However, because of low statistics in the $\gamma$-ray spectra associated with the $s_{1/2}$ ground state state, only the results for the $h_{11/2}$ isomer are presented here. No evidence was found for the $25/2^-$ isomer $\alpha$ line. Figure 6 displays the $\gamma$-ray spectrum tagged by $\alpha$ particles emitted from the $h_{11/2}$ state. The energies, intensities, and angular distribution ratios $R$ for $\gamma$ rays correlated with the $^{157}$Ta $\alpha$ decay are presented in Table II. Gamma rays in coincidence with the strong 842-, 151-, and 643-keV transitions are shown in Fig. 7. The five strongest lines in Fig. 6 are in coincidence with one another. They are proposed to form a single cascade. The 842- and 703-keV lines are noticeably broader than the 643- and 567-keV transitions. This is associated with the presence of an isomer above the first two transitions in the cascade. The $\gamma$ rays below the isomer can be emitted in-flight downstream from the target but still in the view of the Ge detectors, and the broadening is caused by the additional spread in the detection angle. The 151-keV transition is a natural candidate for the isomer deexcitation. Single-particle Weiskopff half-life estimates are about 50 ns and 10 ps for 150-keV E2 and M1 transitions, respectively. This favors an E2 assignment for the 151-keV transition. The E2 conversion coefficient is $\approx$0.7 at 150-keV. The 151 keV transition intensity, corrected for internal conversion, is very close to the intensities of the transitions placed above it. This suggests that most of the $\gamma$ rays below the isomer are emitted close to the target, implying a half-life in the range of 1–10 ns. The transitions in the yrast cascade were ordered according to their intensity.

TABLE II. Energies, intensities, angular distribution ratios, and proposed assignments of the $\gamma$-ray transitions correlated with $\alpha$ decay of the $h_{11/2}$ state in $^{157}$Ta.

| Energy (keV) | Intensity | $R = I_\gamma(\approx 180^\circ)/I_\gamma(\approx 0^\circ)$ | $I^{\pi_i} \rightarrow I^{\pi}{}_f$ assignment |
|---|---|---|---|
| 57.2 | 75.5(69) | | $K_\alpha$ X rays |
| 65.8 | 31.0(41) | | $K_\beta$ X rays |
| 137.7 | 12.1(16) | 0.64(22) | $(31/2^+) \rightarrow (29/2^+)$ |
| 150.6 | 49.6(29) | 0.85(13) | $23/2^- \rightarrow 19/2^-$ |
| 154.7 | 11.8(17) | | |
| 181.0 | 7.9(13) | | |
| 225.3 | 5.4(11) | | |
| 236.2 | 6.6(12) | | |
| 240.3 | 6.2(12) | | |
| 288.5 | 21.8(19) | | |
| 292.6 | 6.9(13) | | |
| 299.5 | 13.1(14) | | |
| 324.2 | 16.7(16) | 0.86(22) | |
| 351.1 | 9.5(14) | | |
| 358.0 | 5.8(12) | | |
| 418.2 | 9.3(14) | | |
| 434.4 | 5.0(12) | | |
| 443.0 | 6.9(14) | | |
| 459.0 | 9.9(16) | | |
| 525.8 | 6.5(15) | | |
| 567.3 | 56.1(33) | 0.86(14) | $(29/2^+) \rightarrow 27/2^-$ |
| 628.1 | 9.5(19) | | |
| 633.0 | 20.2(25) | | |
| 642.6 | 60.9(37) | 0.85(14) | $27/2^- \rightarrow 23/2^-$ |
| 656.9 | 8.2(18) | | |
| 703.2 | 84.4(42) | 1.43(20) | $19/2^- \rightarrow 15/2^-$ |
| 797.3 | 17.7(22) | | |
| 842.0 | 100.0(44) | 1.05(15) | $15/2^- \rightarrow 11/2^-$ |
| 855.0 | 10.7(18) | | |

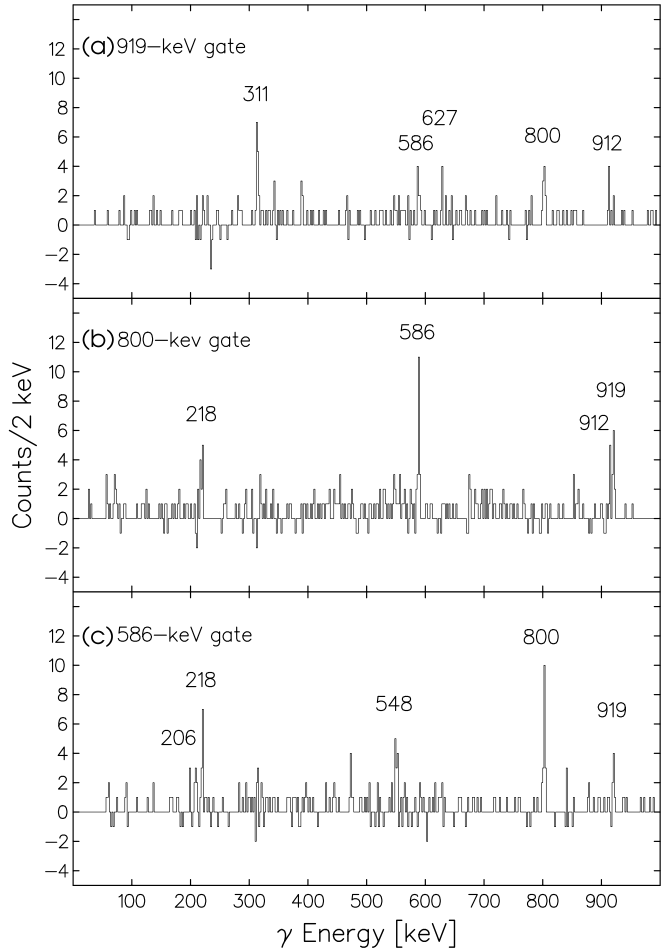


FIG. 4. $\gamma$-ray spectra in coincidence with the 919-, 800-, and 586-keV transitions tagged by the $\alpha$ decay of the $8^+$ isomer in $^{156}$Hf.

The angular distribution coefficients for the 842- and 703-keV lines correspond to that of a stretched quadrupole transition and favor the $15/2^-$ and $19/2^-$ assignments for the 842- and 1545-keV levels. From the above lifetime considerations, $I^\pi = 23/2^-$ is proposed for the 1696 state. The angular distribution ratios for the 643- and 567-keV transitions are ambiguous. Based on systematics, $27/2^-$ and $29/2^+$ quantum numbers are assigned to the 2338- and 2906-keV states, respectively. In addition, the 138- and 289-keV transitions were added at the top of the yrast cascade. Because no evidence was found for another isomer, the 138-keV $\gamma$ ray is likely of M1 character. This is supported by the angular distribution ratio and, hence, spin and parity $31/2^+$ is proposed for the 3043 keV state. A level scheme for $^{157}$Ta is presented in Fig. 8. Only the strongest transitions were placed in the level scheme, because of limited $\gamma\gamma$ statistics.

### C. The $^{158}$W nucleus

The $^{158}$W ground-state decays with the emission of 6442(30)-keV $\alpha$ particles with a 0.9(4)-ms half-life [5]. A line at 8291(24) keV and a 160(50)-$\mu$s half-life was associated with the $8^+$ isomer, analogous to the isomer in $^{156}$Hf [5]. More precise values of 6445(3) keV, 1.5(2) ms and 8286(7) keV, 0.14(2) ms were reported in Ref. [16].

The $\gamma$-ray spectrum tagged by the $\alpha$ particles emitted from the $8^+$ isomer is given in Fig. 9. There are three clusters of counts at 204 keV (4 counts), 478 keV (6 counts), and 1074 keV (3 counts) in the spectrum. Remaining events are scattered over the entire spectrum, indicating large fragmentation of the decay paths similar to $^{156}$Hf. Possible assignments for these three transitions are discussed below.

## III. SHELL-MODEL CALCULATIONS

Shell-model calculations, with the $Z = 64$, $N = 82$ $^{146}$Gd as a core, have been performed using the OXBASH code. The single-particle energies and two-body matrix elements obtained in Ref. [2] were used as input to the calculations. The levels in the even and odd $N = 84$ isotones, including those observed in this work for $^{156}$Hf, $^{157}$Ta, and $^{158}$W, are compared with the results of the shell-model calculations in Figs. 10 and 11, respectively. The calculated states were

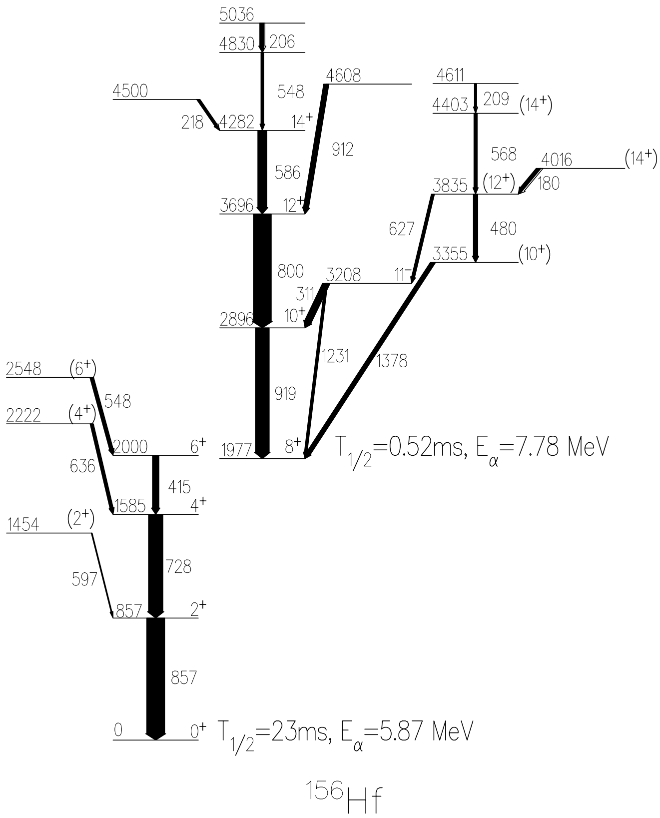


FIG. 5. Proposed $^{156}$Hf level scheme.

divided into two groups corresponding to the $(\nu f_{7/2}h_{9/2})$ and $(\nu f_{7/2})^2$ neutron configurations.

### A. The $^{156}$Hf nucleus

As can be seen in Fig. 10, the energies of the $2^+$, $4^+$, and $6^+$ states in $^{156}$Hf follow the systematics of the lighter even-even $N = 84$ isotones. Based on the shell-model calculations, they are proposed to form the $(\nu f_{7/2})^2$ multiplet together with the ground state. The assignment for the states at 1454, 2222, and 2548 keV is not as clear. There are at least two possibilities. They could be interpreted as the $2^+$, $4^+$, and $6^+$ members of the $h_{9/2}^2$ multiplet. The shell model predicts these states at

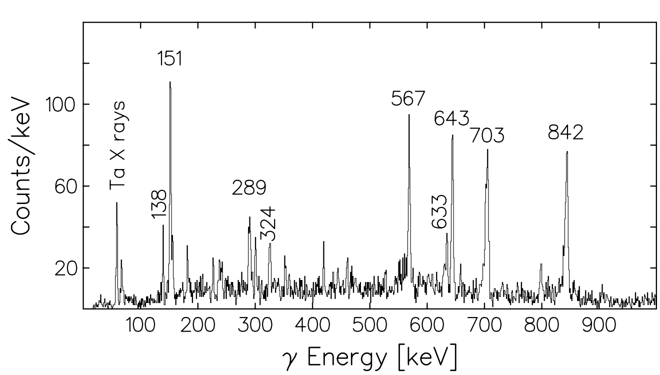


FIG. 6. $\gamma$-ray singles spectrum tagged by the $\alpha$ decay of the $11/2^-$ isomeric state in $^{157}$Ta.

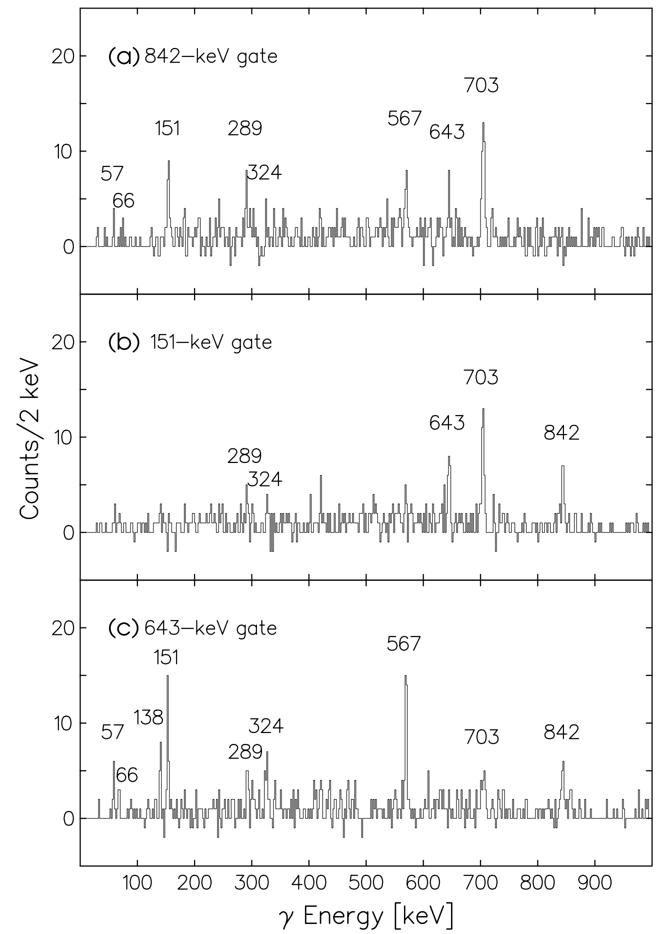


FIG. 7. $\gamma$-ray spectra in coincidence with the 842-, 151-, and 643-keV transitions tagged by the $\alpha$ decay of the $11/2^-$ isomeric state in $^{157}$Ta.

1600, 2000, and 2100 keV, respectively. The 1454-keV state could be also interpreted as an octupole phonon state. Many examples of states based on octupole excitations are known in this region and they are expected to occur as a result of the low octupole phonon energy of 1597 keV in the doubly magic $^{146}$Gd nucleus. However, the energy of the $3^-$ states increases from 1273 keV in $^{148}$Gd to 1524 in $^{152}$Er and can be extrapolated to about 1800 keV in $^{156}$Hf, which makes the latter assignment more doubtful.

As discussed, the $8^+$ isomer has a $\nu f_{7/2}\nu h_{9/2}$ structure. The lowering of the $8^+$ state with respect to the $6^+$ level as $Z$ increases is mainly a consequence of the narrowing of the energy gap between the two lowest lying neutron orbitals, $\nu f_{7/2}$ and $\nu h_{9/2}$. In the heavier $N = 84$ isotones, this trend has been associated with the strong, attractive interaction between the $h_{11/2}$ proton and the $h_{9/2}$ neutron when coupled to spin $I = 1\hbar$ [3]. This attractive interaction occurs for each successive proton pair added to the $^{146}$Gd core. The cascade feeding the $8^+$ isomer resembles the bands feeding the $8^+$ state and the ground-state bands in the lighter $N = 84$ isotones. Consequently, the $8^+$ isomer and the proposed $10^+$, $12^+$, and $14^+$ levels can be interpreted as the $(\nu f_{7/2})^2_{0^+,2^+,4^+,6^+}$ states coupled to the aligned proton pair $(\pi h_{11/2})^2_{10^+}$. According to

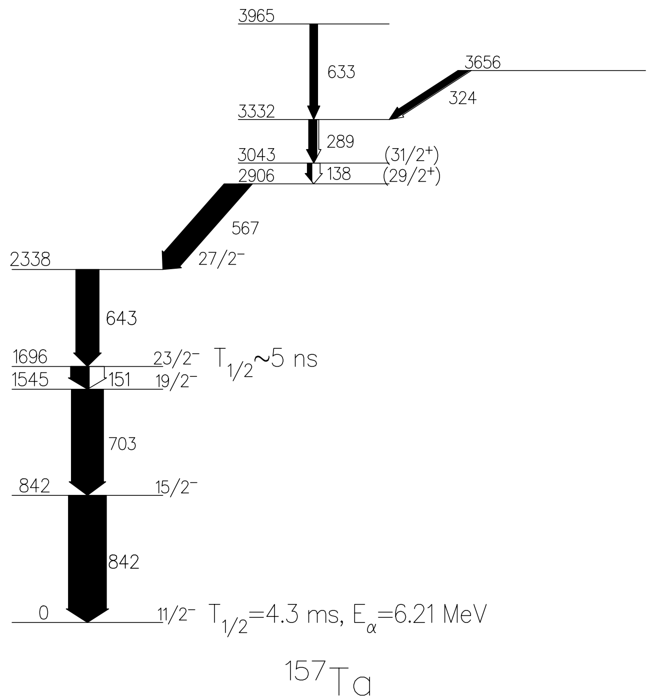


FIG. 8. Proposed $^{157}$Ta level scheme. The level energies are quoted relative to the $h_{11/2}$ isomer. The isomer excitation energy of 22(5) keV was deduced in Ref. [15]. The white portion of the intensity arrows represents the internal conversion contribution.

the shell-model calculations, there are two close-lying $14^+$ states in $^{154}$Yb. Only the $(\nu f_{7/2}\nu h_{9/2})_{14^+}$ level was observed in Ref. [7]. The calculated energy of the $14^+$ state in $^{156}$Hf does not change, in good agreement with experimental observation. The 4500- and 4830-keV states could possibly be the $16^+$ members of the $(\nu f_{7/2})^2$ and $(\nu f_{7/2}\nu h_{9/2})$ multiplets.

The side band can be interpreted as arising from the coupling between the two-neutron multiplets and the octupole excitation. An extensive discussion of octupole excitations in $^{148}$Gd and in neighboring nuclei can be found in Ref. [17]. The state at 3208 keV is located 1231 keV above the $8^+$ isomer.

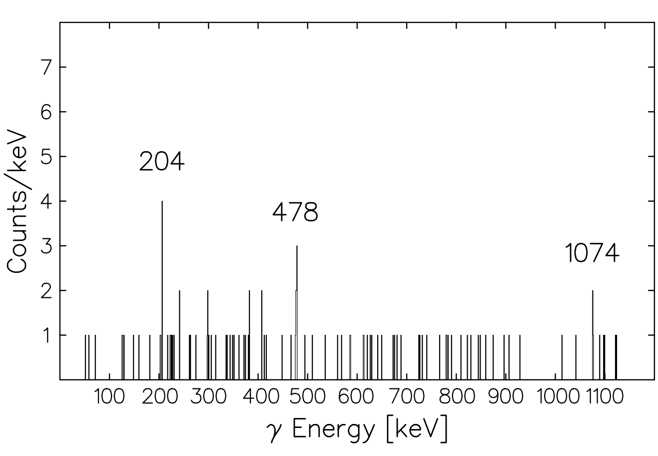


FIG. 9. $\gamma$-ray singles spectrum tagged on the $\alpha$ decay of the $8^+$ isomeric state in $^{158}$W.

This value agrees very well with the separation energies between $(\nu f_{7/2}h_{9/2})_{8^+}$ and $11^-$ states in lighter even-$Z$, $N = 84$ isotones (i.e., 1008, 1070, 1131, and 1181 keV in $^{148}$Gd, $^{150}$Dy, $^{152}$Er, and $^{154}$Yb, respectively). The $11^-$ state has been interpreted in Ref. [17] as resulting from the coupling of the $(\nu f_{7/2}h_{9/2})_{8^+}$ two-neutron configuration to the $3^-$ phonon. This assignment is supported for $^{156}$Hf by the presence of the 1231-keV E3 transition to the $8^+$ state. The $11^-$ state is fed from the 3835-keV level. By analogy to $^{148}$Gd, this level could correspond to a stretched configuration of two $f_{7/2}$ neutrons coupled to two octupole phonons to form a $12^+$ state. In the 4016-keV state, the two neutrons would then be in the $(\nu f_{7/2}h_{9/2})_{8^+}$ configuration instead. In $^{148}$Gd, the $12^+$ and $14^+$ states are separated by 1187 keV, reflecting a much larger gap between the $6^+$ and $8^+$ configurations. The state at 3355 keV could be an analog of the $10^+$ level at 3823 keV in $^{148}$Gd and could, therefore, be regarded as another member of the $\nu f \nu h \otimes 3^+$ multiplet.

Although interpretation of the $^{156}$Hf level structure proposed in this work appears to be quite straightforward, more in depth shell-model analysis may shed light on the higher lying levels and the growing role of the $h_{9/2}$ neutron orbital. A simple extrapolation from known nuclei places this orbital only 200 keV above the $f_{7/2}$ state in $^{156}$Hf, and both orbitals are almost degenerate in $^{158}$W, a nucleus that has only two protons more than $^{156}$Hf. One of the consequences of this degeneracy would be the mixing of the members of the $(\nu h_{9/2})^2_{0^+,2^+,4^+,6^+,8^+}$ multiplet with the yrast states. The shell-model calculations presented here do not take this mixing into account.

### B. The $^{157}$Ta nucleus

The energies of the first two states above the $h_{11/2}$ isomer in $^{157}$Ta are very similar to corresponding values of the 15/2$^-$ and 19/2$^-$ levels in the lighter odd $N = 84$ isotones and the energies of the $2^+$ and $4^+$ states in the even $N = 84$ isotones (see Fig. 11). This supports their interpretation as the $\pi h_{11/2} \otimes (\nu f_{7/2})^2$ configuration. The 23/2$^-$ level at 1696 keV does not follow the increasing trend for the calculated 23/2$^-$ states associated with the $\pi h_{11/2} \otimes (\nu f_{7/2})^2$ stretched configuration. As a result, it is most likely the 23/2$^-$ member of the $\pi h_{11/2} \otimes \nu f_{7/2}h_{9/2}$ multiplet, which, according to the calculations, drops down rapidly in energy with decreasing mass. The 27/2$^-$ state feeding the 23/2$^-$ level has the same configuration and is maximally stretched. In $^{155}$Lu [10], the 25/2$^-$ state corresponding to the same configuration is a yrast trap and is isomeric. No evidence for the $\alpha$ decay of this state was found in the data. It is plausible that the 23/2$^-$ state intercepts most of the flux in $^{157}$Ta. The energy of the 27/2$^-$ level is slightly higher than that in $^{155}$Lu, in contrast to the slowly decreasing trend exhibited by the shell-model calculations.

The lowering of the 23/2$^-$ level with respect to the $\pi h_{11/2} \otimes (\nu f_{7/2})^2$ multiplet reflects the drop in energy of the $\nu h_{9/2}$ orbital with respect to the $\nu f_{7/2}$ state. The 27/2$^-$ state is a maximum-spin, seniority-1 state and the $(\pi h_{11/2} \otimes \nu h_{9/2})_{1^+}$ strong attractive interaction is blocked in this state, whereas in

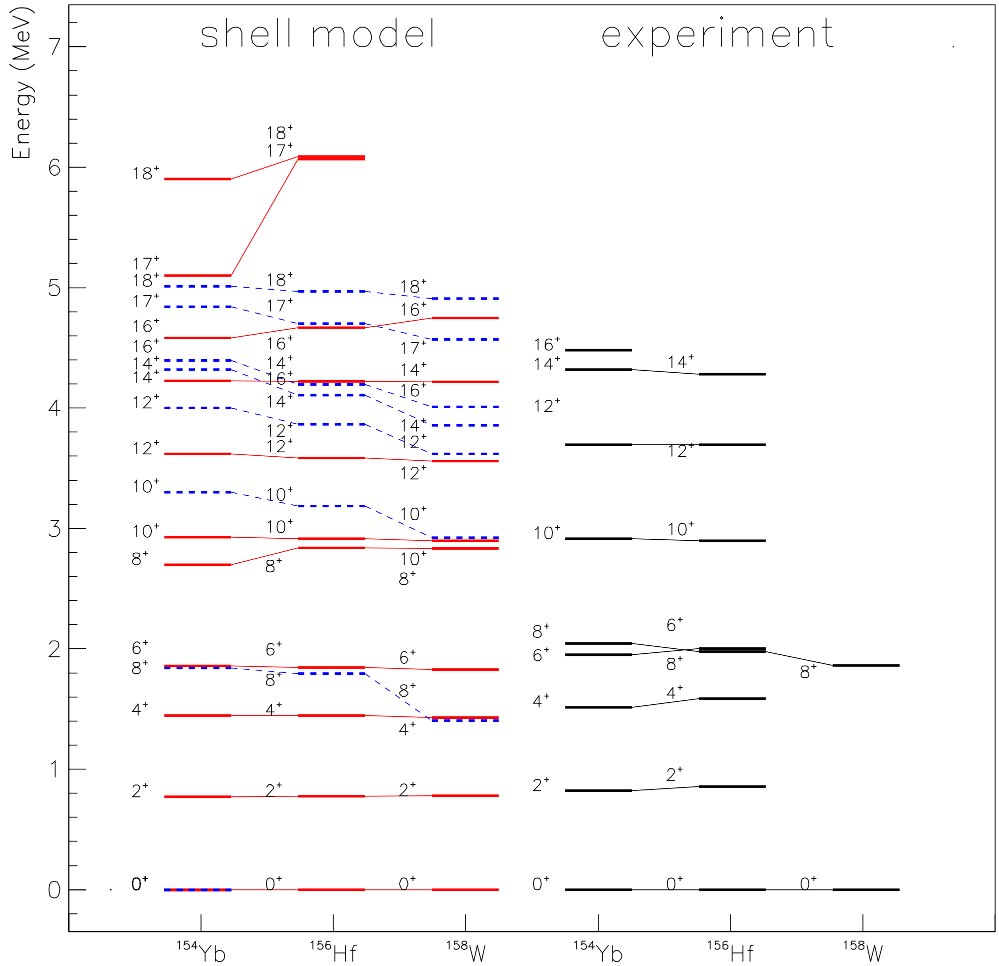


FIG. 10. (Color online) Comparison between the yrast states observed in the even-even $N = 84$ isotones and the results of the shell-model calculations discussed in the text. The calculated levels based on the $(\nu f_{7/2})^2$ and the $\nu f_{7/2}h_{9/2}$ configuration are marked as solid and dashed lines, respectively.

the $23/2^-$ state, which has one additional broken proton pair, protons can couple with the $h_{9/2}$ neutron to spin $1\hbar$.

In lighter odd $N = 84$ isotones, the $27/2^-$ state is fed primarily from the $29/2^+$ state, which was assigned as the $\pi h_{11/2} \otimes [(\nu f_{7/2})^2 \otimes 3^- + \nu f_{7/2} i_{13/2}]$ configuration; see, for example, $^{153}$Tm [8]. By the same token, the 3332-keV level could correspond to the $\pi h_{11/2} \otimes \nu f_{7/2} i_{13/2}$ stretched state. The splitting between the $29/2^+$ and $31/2^+$ states increases in heavier isotones, which can be associated with the increasing energy of the $i_{13/2}$ state.

### C. The $^{158}$W nucleus

According to the shell-model calculations, the $10^+$ and $12^+$ states based on the $(\nu f_{7/2})^2$ and $\nu f_{7/2}h_{9/2}$ configurations have similar excitation energies. The calculated $14^+$ and $16^+$ states originating from the $\nu f_{7/2}h_{9/2}$ multiplet are located below the $[(\pi h_{11/2})^2 \otimes (\nu f_{7/2})^2]_{14^+}$ configuration. Comparison with the shell model results suggests that the 1074-, 478-, and 204-keV transitions could correspond to the $10^+ \to 8^+$, $14^+ \to 12^+$, and $16^+ \to 14^+$ transitions, respectively, with the $14^+ \to 12^+$ transition remaining undetected. Alternatively, the 204-keV $\gamma$ line could correspond to the $11^- \to 8^+$ transition. Clearly, another experiment with the beam energy optimized for the $2n$ evaporation channel is necessary to establish the $^{158}$W level scheme above the ground state and the $8^+$ isomer.

## IV. SUMMARY

In conclusion, results for excited states in three $N = 84$ isotones, $^{156}$Hf, $^{157}$Ta, and $^{158}$W, are presented for the first time in this work. The proposed $\gamma$-ray transitions were unambiguously assigned to the individual reaction channels using the RDT method. The resulting level schemes, to a large extent, follow the systematics of the lower-$Z$ $N = 84$ isotones. States involving octupole vibrations were found in $^{156}$Hf. The agreement between the deduced level schemes and shell model calculations is quite good, but worsens as the number of protons increases. This might indicate that the $(h_{9/2})^2$ multiplet plays an increasing role and should be included in the calculations.

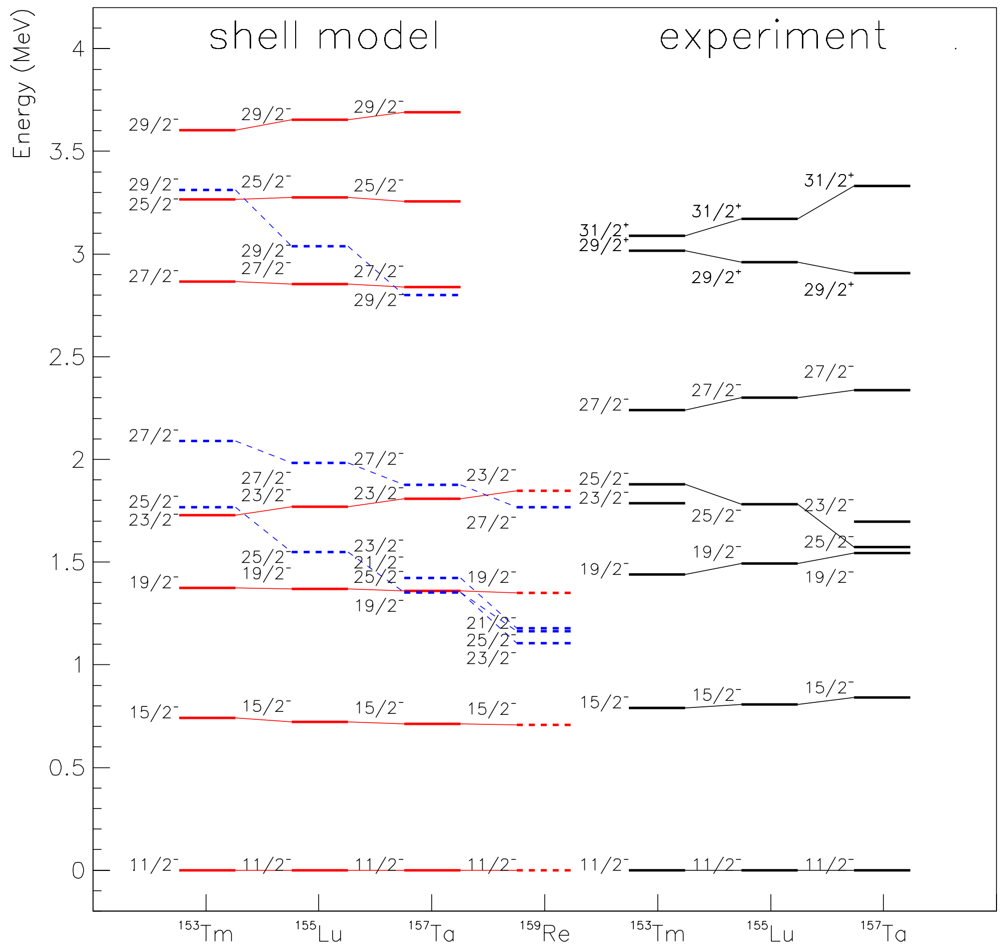


FIG. 11. (Color online) Comparison between the states observed in the odd $N = 84$ isotones and the results of the shell-model calculations discussed in the text. The calculated levels based on the $(\nu f_{7/2})^2$ and the $\nu f_{7/2}h_{9/2}$ configuration are marked as solid and dashed lines, respectively. The $\alpha$ decay of the $25/2^-$ isomer in $^{157}$Ta was not observed in the present work and the excitation energy derived from the $\alpha$ energy reported in Ref. [5] was adopted in the figure.

## ACKNOWLEDGMENTS

This work is supported by the U.S. Department of Energy, Office of Nuclear Physics, under contract no. W-31-109-ENG-38 and by the National Science Foundation. P.J.W. wish to acknowledge travel support from NATO under Grant CRG 940303.

[1] P. Kleinheinz, R. Broda, P. J. Daly, S. Lunardi, M. Ogawa, and J. Blomqvist, Z. Phys. A **290**, 279 (1979).
[2] M. Lach, P. Kleinheinz, M. Piiparinen, M. Ogawa, S. Lunardi, M. C. Bosca, J. Styczen, and J. Blomqvist, Z. Phys. A **341**, 25 (1991).
[3] C. T. Zhang, P. Kleinheinz, M. Piiparinen, R. Broda, R. Collatz, P. J. Daly, K. H. Maier, R. Menegazzo, G. Sletten, J. Styczen, and J. Blomqvist, Phys. Rev. C **54**, R1 (1996).
[4] P. J. Woods and C. N. Davids, Annu. Rev. Nucl. Part. Sci. **47**, 541 (1997).
[5] R. D. Page, P. J. Woods, R. A. Cunningham, T. Davinson, N. J. Davis, A. N. James, K. Livingston, P. J. Sellin, and A. C. Shotter, Phys. Rev. C **53**, 660 (1996).
[6] J. H. McNeill, J. Blomqvist, A. A. Chishti, P. J. Daly, W. Gelletly, M. A. C. Hotchkis, M. Piiparinen, B. J. Varley, and P. J. Woods, Phys. Rev. Lett. **63**, 860 (1989).
[7] C. T. Zhang, R. Broda, R. Menegazzo, P. Kleinheinz, R. Collatz, H. Grawe, S. Hofmann, M. Lach, K. H. Maier, M. Schramm, R. Schubart, and J. Blomqvist, Z. Phys. A **345**, 327 (1993).
[8] C. T. Zhang, P. Kleinheinz, M. Piiparinen, R. Collatz, T. Lonnroth, G. Sletten, and J. Blomqvist, Z. Phys. A **348**, 249 (1994).
[9] D. Seweryniak *et al.*, *Proceedings of the Conference on Nuclear Structure at the Limits*, Argonne, 1996, ANL/PHY-97/1, 1997, p. 247.
[10] K. Y. Ding *et al.*, Phys. Rev. C **64**, 034315 (2001).
[11] I. Y. Lee, Nucl. Phys. **A520**, 641c (1990); R. V. F. Janssens and F. S. Stephens, Nucl. Phys. News **6**, 9 (1996).

[12] C. N. Davids *et al*., Nucl. Instrum. Methods B **70**, 358 (1992).

[13] E. S. Paul, P. J. Woods, T. Davinson, R. D. Page, P. J. Sellin, C. W. Beausang, R. M. Clark, R. A. Cunningham, S. A. Forbes, D. B. Fossan, A. Gizon, J. Gizon, K. Hauschild, I. M. Hibbert, A. N. James, D. R. LaFosse, I. Lazarus, H. Schnare, J. Simpson, R. Wadsworth, and M. P. Waring, Phys. Rev. C **51**, 78 (1995).

[14] S. Hofmann, P. Armbruster, G. Berthes, T. Faestermann, A. Gillitzer, F. P. Hesberger, W. Kurcewicz, G. Münzenberg, K. Poppensieker, H. J. Schott, and I. Zychor, Z. Phys. A **333**, 107 (1989).

[15] R. J. Irvine *et al*., Phys. Rev. C **55**, R1621 (1997).

[16] H. Mahmud, C. N. Davids, P. J. Woods, T. Davinson, D. J. Henderson, R. J. Irvine, D. Seweryniak, and W. B. Walters, Phys. Rev. C **62**, 057303 (2000).

[17] M. Piiparinen, P. Kleinheinz, S. Lunardi, M. Ogawa, G. de Angelis, F. Soramel, W. Meczynski, and J. Blomqvist, Z. Phys. A **337**, 387 (1990).